Supporting Information for:

The Basic Equations Under Weak Temperature Gradient Balance: Formulation, Scaling, and Types of Convectively-coupled Motions

Ángel F. Adames

Department of Atmospheric and Oceanic Sciences, University of Wisconsin, Madison, Wisconsin

Corresponding author: Ángel F. Adames, angel.adamescorraliza@wisc.edu

ABSTRACT: This document contains additional information for the manuscript titled "The Basic Equations Under Weak Temperature Gradient Balance: Formulation, Scaling, and Types of Convectively-coupled Motions"

1. Using potential temperature instead of DSE to define WTG balance

The thermodynamic equation in terms of potential temperature (θ) can be written as:

$$\frac{DC_p\theta}{Dt} = \frac{Q}{\Pi} \tag{1}$$

where

$$\Pi = \left(\frac{p}{p_s}\right)^{\frac{R_d}{C_p}} \tag{2}$$

is the Exner function. The component of the circulation that obeys strict WTG balance using θ is written as:

$$\mathbf{u}_w \cdot \nabla C_p\theta \equiv \frac{Q}{\Pi} \tag{3}$$

and the non-WTG residual as

$$\frac{\partial\theta}{\partial t} + \mathbf{u}' \cdot \nabla\theta = 0. \tag{4}$$

Conventionally, PV is defined using potential temperature. To keep the same units as the PV definition in the main text, we define the θ-based PV by multiplying by C_p, yielding the following:

$$\mathrm{PV} = -g\boldsymbol{\eta}_a \cdot \nabla C_p\theta. \tag{5}$$

The PV budget takes the following form:

$$\frac{D\mathrm{PV}}{Dt} = -g\boldsymbol{\eta}_a \cdot \nabla\left(\frac{Q}{\Pi}\right). \tag{6}$$

Lastly, the WTG moisture budget can be written using a θ-based definition of the WTG circulation:

$$\frac{\partial Lq}{\partial t} = -(\mathbf{u}' + \mathbf{u}_r) \cdot \nabla Lq - \Pi\mathbf{u}_c \cdot \nabla C_p\theta_e - \Pi\frac{\partial F_m}{\partial p}. \tag{7}$$

where we have used the approximate form of the equivalent potential temperature (θ_e):

$$C_p\theta_e \simeq C_p\theta + \frac{Lq}{\Pi}. \tag{8}$$

Note that using θ instead of DSE to define the WTG thermodynamic and moisture equations leads to similar results, except the Exner function appears in several terms. This result implies that the DSE and $C_p\theta$ are interchangeable in the lower troposphere, where $\Pi \simeq 1$, but their differences become larger in the upper troposphere. Generally, moisture fluctuations are small in this layer, so that the DSE budget can be used in place of θ to obtain a simpler moisture budget. However, the errors that arise from using DSE can be important if one is seeking high accuracy.

2. The WTG approximation and the PV impermeability theorem

To better understand how WTG balance and its departure affects the evolution of PV we invoke the impermeability theorem (Haynes and McIntyre 1990). Let us consider two concentric spheres that are made out of isentropic surfaces, neither which intersect the ground, as depicted in Fig. 1a in the main text. The average amount of PV that is found between these two isentropic surfaces is:

$$\{\mathrm{PV}\} = \frac{1}{\mathcal{A}(s_2 - s_1)} \oiint_{\mathcal{A}} \int_{s_1}^{s_2} \mathrm{PV} ds d\mathcal{A} \tag{9}$$

where $\mathcal{A}$ is the average area of Earth. We have assumed that the two isentropic layers have similar area because the depth of the troposphere is much smaller than the radius of Earth. Because the integral boundaries do not change with time, we can write the budget equation for {PV} as:

$$\frac{\partial\{\mathrm{PV}\}}{\partial t} = \frac{1}{\mathcal{A}(s_2 - s_1)} \oiint_{\mathcal{A}} \int_{s_1}^{s_2} \boldsymbol{\nabla}\cdot\mathbf{J}\, ds d\mathcal{A} \tag{10}$$

We now use the divergence theorem to evaluate the integrals in Eq. (13) along the two isentropic surfaces only:

$$\oiint_{a} \int_{s_1}^{s_2} \mathrm{PV} ds d\mathcal{A} = \oiint_{s_1} (s\boldsymbol{\eta}_a)\cdot\mathbf{n} d\mathcal{A} + \oiint_{s_2} (s\boldsymbol{\eta}_a)\cdot\mathbf{n} d\mathcal{A} \tag{11}$$

where the subscript in each integral describes the isentropic surface that is being evaluated and $\mathbf{n}$ is a unit vector that is normal to these surfaces. Because the integrals on the rhs of Eq. (11) are evaluated along surfaces of constant s, it follows that we can take s out of the integral:

$$\oiint_{s_1} (s\boldsymbol{\eta}_a)\cdot\mathbf{n}\,d\mathcal{A} = s_1 \oiint_{s_1} \boldsymbol{\eta}_a\cdot\mathbf{n}\,d\mathcal{A} \tag{12}$$

and the same is done for the surface s_2. After doing this, we can once again invoke the divergence theorem but evaluating it along the volume that is encompassed by each individual isentropic surface, i.e.

$$\oiint_{s_1} \boldsymbol{\eta}_a\cdot\mathbf{n}\,d\mathcal{A} = \iiint_{V(s_1)} \boldsymbol{\nabla}\cdot\boldsymbol{\eta}_a dV = 0. \tag{13}$$

Because the absolute vorticity vector is non-divergent by definition, it follows that the two volume integrals are zero. As a result $\{\mathrm{PV}\} = 0$ and hence both sides of Eq. (10) must also be zero.

When evaluating the rhs of Eq. (10), we see that the vector $\mathbf{J}_w$ is always parallel to the isentropic surface and hence vanishes. Because the concentric spheres are assumed to be parallel to the Earth's surface, we can evaluate the integral as follows:

$$\oiint_{\mathcal{A}} \int_{s_1}^{s_2} \boldsymbol{\nabla}\cdot\mathbf{J}\,ds\,d\mathcal{A} \simeq \oiint_{s_2} \omega'\mathrm{PV}d\mathcal{A} - \oiint_{s_1} \omega'\mathrm{PV}d\mathcal{A} = 0 \tag{14}$$

Thus, the non-WTG flow cannot flux of PV across the isentropic surfaces. It can, however, flux mass, as discussed by Haynes and McIntyre (1987, 1990). By moving the isentropic surfaces, PV can be concentrated locally, even though $\{\mathrm{PV}\}$ remains unchanged, as also discussed in Vallis (2017).

3. Defining the gravity wave phase speed

Our definition of the gravity wave phase speed can be obtained by considering the equations of motions (Eq. 4 in the main text) in a dry atmosphere when $\mathrm{Ro}_\tau \gg 1$, which yields the following system of equations:

$$\frac{\partial \mathbf{v}}{\partial t} = -\nabla_h \Phi' \tag{15a}$$

$$\frac{\partial u}{\partial x} + \frac{\partial v}{\partial y} + \frac{\partial \omega}{\partial p} = 0 \tag{15b}$$

$$\frac{\partial}{\partial t}\left(\frac{\partial \Phi'}{\partial p}\right) = -\omega\sigma \tag{15c}$$

where

$$\sigma = \frac{R_d S_p}{p c_p} \tag{16}$$

can be thought of as a static stability parameter. Equation (15) can be combined to form the following :

$$\frac{\partial}{\partial t}\left(\frac{\partial}{\partial p}\frac{1}{\sigma}\frac{\partial}{\partial p}\right)\Phi' = -\nabla_h^2\Phi'. \tag{17}$$

If σ is assumed to be constant, Eq. (17) simplifies to the wave equation for a wave with a vertical wavenumber m, and its solution corresponds to a gravity wave with a phase speed of $c = \sqrt{\sigma}/m$. This solution is identical to the gravity wave speed scaling used in Eq. (44) of the main text if P is assumed to correspond to m^{-1}.

4. Comparing the N_{mode} defined in this study with the definition of Adames et al. (2019)

The definition of N_{mode} in Eq. (62) of the main text is very similar to the one found by Adames et al. (2019). In their shallow water model, $\mathrm{N}_{mode} = \mathrm{Fr}_\tau^2/[N_c(1-\tilde{M})]$, where $\tilde{M}$ is the gross moist stability, and N_c is the ratio between the convective moisture adjustment timescale (τ_c) and τ. Interestingly, Adames et al. (2019) found that N_c exhibits a near-constant value for motion systems with different spatial and temporal scales. We can show that this is indeed the case if we define τ_c as the ratio between the convective heating scaling Q_c and the moisture scaling Lq, yielding $\tau_c = L\mathrm{q}/\mathrm{Q}_c$. Assuming that the two definitions of N_{mode} are equivalent, we can combine them to find that:

$$\tau_c \sim \tau(1-\hat{\alpha}) \tag{18}$$

which shows that τ_c/τ is approximately constant if $\hat{\alpha}$ does not vary much in time and space. Close examination of Eq. (18) reveals that τ_c is longer for slowly evolving tropical motion systems. It is also shorter in more humid environments since stronger convection in these regions will dry the column more quickly.

5. Description of the simple vortex

In order to construct the simple vortex shown in Fig. 6 of the main text, we assumed a gaussian geopotential distribution

$$\Phi' = \Phi_0 \exp\left(b\left[(x^2+y^2\right]\right) \tag{19}$$

where $\Phi_0 = 5\ \text{m}^2\ \text{s}^{-2}$, $b = 4\times 10^{-11}\ \text{m}^{-2}$ is a constant that describes the decay rate of the geopotential. We assume that the vortex is in gradient wind balance, and thus can be diagnosed from the geopotential as follows:

$$V' = -\frac{fr}{2} + \frac{r}{2}\left(f^2 - 8b\Phi'\right)^{\frac{1}{2}} \tag{20}$$

where $r = \sqrt{x^2+y^2}$, and f is the planetary vorticity whose value at 15°N is the value we use at the center of the vortex. We can obtain u' and v' from V' by going from polar coordinates to Cartesian coordinates:

$$u' = -V' \sin(\varphi) \qquad\qquad v' = V' \cos(\varphi) \tag{21}$$

where

$$\varphi = \tan^{-1}\frac{y}{x} \tag{22}$$

Lastly, we also use a Gaussian for the distribution of χ_w:

$$\chi_w = \chi_0 \exp\left(b\left[(x-\tilde{x}_0)^2 + (y-\tilde{y}_0)^2\right]\right) \tag{23}$$

where $\chi_0 = 2.5\times 10^4\ \text{m}^2\ \text{s}^{-1}$, $x_0 = -100$ km and $y_0 = -50$ km.

Figure 1 shows the same distribution of terms as in Fig. 6 in the main text but for the case in which $x_0 = y_0 = 0$, that is, the convergence is co-located with the vorticity. While panels (c) and (d) are different from Fig. 6 in the main text only in their horizontal displacement, we see some differences in panels (b) and (e). Because the convergence is centered at the center of the vortex, $\mathbf{v}'$ does not contribute to the convergence of the divergence flux – it is driven purely by the component of the flow that is in exact WTG balance. Furthermore, because χ and ψ have the same structure and are co-located, the term det($\mathbf{A}$) is zero. The sum of all the terms reveals a convergence tendency at the center of the vortex, flanked by a positive divergence tendency. The beta effect causes the ring of divergence to exhibit an asymmetry, and we also see a weak positive convergence tendency to the west of the center of circulation.

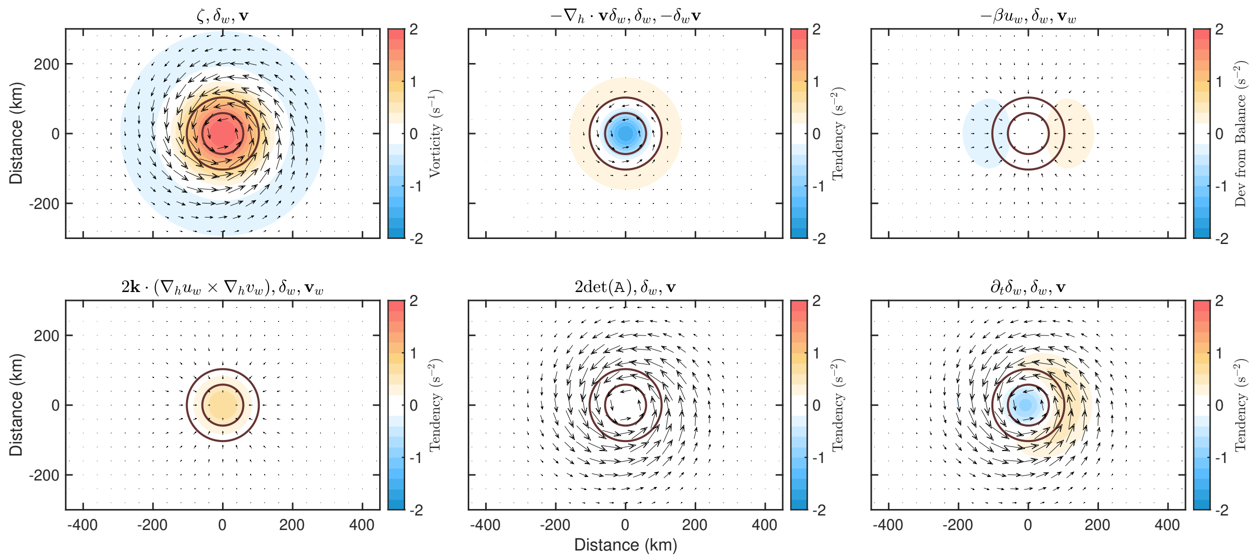

FIG. 1. As in Fig. 6 in the main text except both ζ and δ_w are centered at $x = y = 0$.

6. WTG equations with friction

In the main text we simplified the basic equations and obtained the "WTG equations" for inviscid flow. Friction was not considered in order to avoid additional complications to the analysis and because finding scaling values for this term in the free troposphere can be challenging (see Kim and Zhang 2021). Nonetheless, it is useful to show how the WTG equations would look like if friction is included. In Eulerian form they are written as:

$$\frac{\partial \zeta}{\partial t} = -\boldsymbol{\nabla}_h \cdot (\mathbf{v}\zeta_a - \omega_w \boldsymbol{\eta}_h + \mathbf{k} \times \mathbf{F}_r) \tag{24a}$$

$$\frac{\partial \delta_w}{\partial t} = -\boldsymbol{\nabla}_h \cdot \left(\mathbf{v}\delta_w + \omega_w \frac{\partial \mathbf{v}}{\partial p} + \mathbf{F}_r \right) - \Sigma \tag{24b}$$

where $\mathbf{F}_r$ is the frictional force, including the effects of turbulent processes. In Lagrangian form the equations can be written as:

$$\frac{D\zeta_a}{Dt} = \boldsymbol{\eta}_a \cdot \boldsymbol{\nabla}\omega_w - \boldsymbol{\nabla}_h \cdot (\mathbf{k} \times \mathbf{F}_r) \tag{25a}$$

$$\frac{D\omega_w}{Dt} = \{\Sigma\} + 2\left\{\frac{\partial \mathbf{u}}{\partial p} \cdot \nabla \omega_w\right\} - \nabla_h \cdot \mathbf{F}_r \tag{25b}$$

References

Adames, Á. F., D. Kim, S. K. Clark, Y. Ming, and K. Inoue, 2019: Scale Analysis of Moist Thermodynamics in a Simple Model and the Relationship between Moisture Modes and Gravity Waves. *Journal of the Atmospheric Sciences*, **76 (12)**, 3863–3881, doi:10.1175/JAS-D-19-0121.1.

Haynes, P. H., and M. McIntyre, 1990: On the conservation and impermeability theorems for potential vorticity. *Journal of Atmospheric Sciences*, **47 (16)**, 2021–2031.

Haynes, P. H., and M. E. McIntyre, 1987: On the evolution of vorticity and potential vorticity in the presence of diabatic heating and frictional or other forces. *Journal of Atmospheric Sciences*, **44 (5)**, 828 – 841, doi:10.1175/1520-0469(1987)044<0828:OTEOVA>2.0.CO;2.

Kim, J.-E., and C. Zhang, 2021: Core dynamics of the mjo. *Journal of the Atmospheric Sciences*, **78 (1)**, 229–248.

Vallis, G. K., 2017: *Atmospheric and oceanic fluid dynamics*, Vol. 2. Cambridge University Press.